Int. J. Heat Mass Transfer. Vol. 30, No. 1, pp. 187–197, 1987
Printed in Great Britain

0017–9310/87 $3.00 + 0.00
Pergamon Journals Ltd.

Radiation heat transfer in foam insulation

L. GLICKSMAN,* M. SCHUETZ† and M. SINOFSKY‡

* Department of Mechanical Engineering, Massachusetts Institute of Technology, Cambridge, MA 02139, U.S.A.
† Owens Corning Fiberglas Technical Center, Granville, OH 43023, U.S.A.
‡ ChemFab Corporation, Buffalo, NY 14221, U.S.A.

(*Received* 15 *September* 1985 *and in final form* 7 *May* 1986)

Abstract—The contribution of radiation heat transfer to the overall conductivity of foam insulations has been examined. The absorption and scattering coefficients as well as the phase function were measured for foam and glassfiber insulation. A simple absorption coefficient can be derived from transmissivity measurements over a range of sample thickness. When this absorption coefficient is used in the diffusion equation to predict the radiative flux for foams, the error in the calculated radiant flux is of the order of ten percent for foams. For fibrous insulation, transmissivity measurements with an integrating sphere are necessary.

BACKGROUND

THIS work is part of an ongoing comprehensive study of heat transfer and aging in closed-cell foam insulation at the Massachusetts Institute of Technology. References [1, 2] deal with diffusion and overall heat transfer, respectively, in foam insulations. The present paper will concentrate on the radiative contribution to heat transfer in foam. While most of the experiments were performed on commercial polyurethane foam insulation, the results should be applicable to all polymeric foam insulations.

Previous published studies have held that radiation in foam is not important. Both Skochdopole [3] and Doherty *et al.* [4] assume that the cell walls are opaque to radiation and calculate a very modest radiant heat flux for foams with reasonable cell sizes. Valenzuela [5] recently pointed out discrepancies between measured and predicted conductivities when using the opaque wall model.

Williams *et al.* [6] recognized that the cell walls are highly transparent. However, their model for radiation in foams neglects the struts formed at the intersection of cell walls. Reitz [2] reported that the cell membranes contain only 10–20% of the solid, with the struts accounting for 80–90%.

There are extensive references in the heat transfer literature dealing with the general problem of simultaneous conduction and radiation in an emitting, absorbing and anisotropic scattering medium which are applicable to the problem of heat transfer in foam. Exact numerical solutions and approximate analytical solutions exist for many problems of practical importance. However, the solutions require knowledge of material properties for which little or no data exists.

Very little information exists on the extinction coefficient or absorption coefficient for foams, and the authors were unable to find any measurements of the scattering characteristics of insulations. In addition, there is little understanding of what property measurements must be made, or what accuracy is required for accurate prediction of the radiative transfer in fibrous or foam insulations. Experimental data on the magnitude of the radiative properties are also needed to determine if simpler limiting forms of the radiative transfer expressions are applicable to insulations. The goals of this work are to provide information concerning the radiative properties of insulation, especially foams, to provide a model to predict radiative transfer, and to establish a simple but accurate means to measure the needed property.

MEASUREMENT OF THE TRANSMISSIVITY OF CELL WALLS

As a first step in dealing with radiation through foam, the transmissivity of cell walls was measured to determine if the cell wall is opaque, as has been implied in earlier work. Since the optical characteristics of the polymer in the cell wall may be influenced by its structure and its forming history, samples of cell walls were used in the experiment rather than continuous films of the polymer formed by different operations. Polyurethane films were obtained from two sources: free rise buns and specially designed foams. Large surface bubbles (up to 2 cm in diameter) were formed on the tops of cast foam samples which were allowed to rise unconstrained. The bulk foam, below the surface in these samples, had a density of about 33 kg m^{-3} and a cell size of 1 mm. A second technique involved the creation of foams with a mean cell size of approximately 0.5 cm. It was possible to locate and remove some films up to 1.0 cm in diameter. The chemical composition and structure of both of these films are representative of typical commercial polyurethane and polyisocyanerate foams. Note that the typical cell diameter of commercial foams is much smaller than this special large cell foam.

NOMENCLATURE

e	emissive power
F	forward fraction, equation (14)
I	intensity
I_0	incident intensity
k_c	conductivity in absence of radiation
k_{eff}	effective conductivity of medium
K_λ	monochromatic extinction coefficient
K^*	weighted extinction coefficient, equation (12)
K_{app}	apparent or measured extinction coefficient
K_R	Rosseland mean absorption coefficient
q	heat flux
s	pathwise coordinate
t	thickness
T	temperature
x	coordinate.

Greek symbols

α	absorption coefficient
θ	polar angle
σ	Stefan–Boltzmann constant
σ_s	scattering coefficient
σ_s^*	scaled scattering coefficient, equation (10)
τ	percent transmission
Φ	phase function
ω	solid angle
ω'	incident solid angle
Ω	albedo
$\langle\cos\theta\rangle$	asymmetry factor, equation (11)

Subscripts

a	apparent or measured
b	black body
r	radiative
T	total
λ	at wavelength λ
L	of the laser beam
$P-1$	weighted, equations (10)–(12).

Figure 1 presents the transmission of infra-red radiation through polyurethane films obtained from both sources. The measurements were taken on a Perkin–Elmer 283B Infra-red Spectrophotometer. Note that at room temperature 89% of black-body energy is emitted between 5 and 32 μm wavelength. These are the important wavelengths for radiant transfer through foam at room temperature.

The free rise bun film was much thinner (1.5 μm) than the film from large cell foam (36 μm). By scanning electron micrograph examination of polyurethane foams, Reitz found the typical cell membrane thickness in commercial foams to be approximately 0.5 μm [2]. Therefore, cell membranes will have even higher transmissivities than the samples in Fig. 1, and the opaque cell wall radiation model is inappropriate. Since the cell walls are not totally transparent, a significant number of cells is required for appreciable absorption (or emission) of radiant energy. Because of the small cell size (approximately 0.5–1 mm), a typical foam board is many cells thick. Thus, a continuum model with the foam as a semi-transparent body is appropriate.

In general, insulation can emit radiant energy, it can absorb radiant energy emitted from the boundaries and from other locations within the foam; in addition it can scatter incident energy. To characterize different insulations, the scattering and absorption behavior of the foam must be measured.

For radiant energy traversing a volume of insulation in a given solid angle at wavelength, λ, the decrease in intensity can be related to the extinction coefficient:

$$\frac{dI_\lambda}{dx} = -K_\lambda I_\lambda = -\alpha_\lambda I_\lambda - \sigma_{s\lambda} I_\lambda \tag{1}$$

where α_λ and $\sigma_{s\lambda}$ are the absorption and scattering coefficient, respectively, and the sum is the extinction coefficient, K_λ. The amount of radiant energy emitted in the same distance dx can be found as $\alpha_\lambda I_{b\lambda}$ where $I_{b\lambda}$ is the black-body intensity at the local temperature of the insulation. In general, an increase in intensity should be included due to emission and in-scattering, see below.

The scattering of radiant energy is further characterized by the phase function, $\Phi_\lambda(\theta)$, which is the ratio of the intensity of scattered energy in a given direction, θ, to the intensity if the scattering is isotropic, i.e. scattered equally in all directions. The angle, θ, is measured relative to the direction of the incident energy before it is scattered.

EXPERIMENT

A complete characterization of the radiative properties of a material requires measurement of the absorption coefficient, scattering coefficient, and phase function for each wavelength. Experiments were undertaken to obtain representative values of these properties for foam insulation.

To measure the extinction coefficient, the foam was sliced into approximately 6–8 samples ranging from a maximum thickness of 2.54 mm (0.1 in.), approximately 3–5 cell diameters thick, to the thinnest slice which did not crumble. Special care was taken to obtain thin samples by carefully slicing the foam using

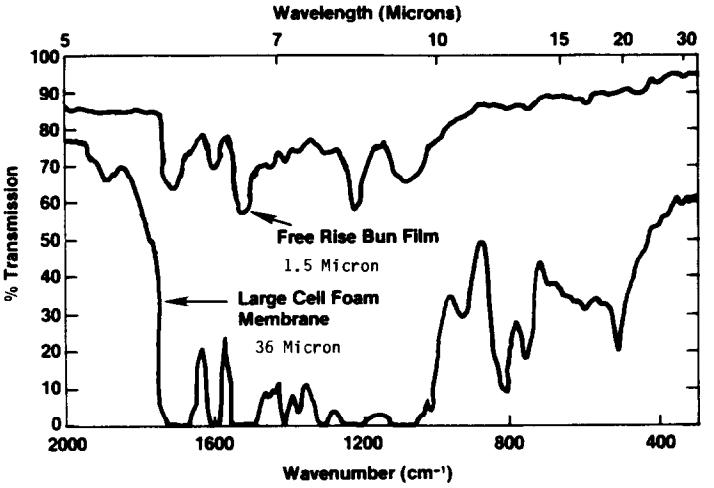

FIG. 1. Transmission of radiation through a single polyurethane cell wall.

a surgeon's scalpel. Thicker slices were obtained using a commercial meat slicer. The slices were individually placed in a conventional infra-red spectrometer (Perkin–Elmer 283B) to measure the transmission from 2.5 to 40 μm wavelength. The sample was placed normal to the source beam.

The thickness of each foam slice was measured with a Lufkin paper micrometer. The paper micrometer has two flat measuring surfaces, attached to the ends of the spindle and caliper. These surfaces are much larger in diameter than the spindle on a conventional micrometer, eliminating local compression of the sample. The uncertainty in thickness measurements is approximately ± 0.025 mm.

The extinction coefficient is calculated by breaking the spectrum into wavelength bands over which the transmission is approximately constant. The slope of $\ln(\tau)$ vs thickness is the extinction coefficient for that wavelength band.

SCATTERING

The monochromatic scattering properties, $\sigma_{s\lambda}$ and $\Phi(\theta)$, were measured for foam and fiberglass at a single wavelength. A schematic diagram of the apparatus is shown in Fig. 2. The beam was generated by a CO_2 laser at a wavelength of 9.64 μm. The laser beam was directed through a chopper to produce a square wave from the continuous output laser. A zinc selenide window was used as a mirror to reduce the power level of the source beam. The beam was incident on the sample at the pivot point of the detector bracket. The detector, a liquid-nitrogen-cooled photoconducting type detector, had a gold-doped germanium sensing element. This provided a clean square wave output signal at the chopping frequency of 395 ± 10 Hz. The lock-in amplifier synchronized to the chopper provided a maximum gain of 10^6. The detector was rotated around the pivot point to measure the energy from the sample as a function of angle from the direction of the incident beam. A thermopile detector was used to calibrate the incident laser power. The laser power output drifted with time, requiring frequent recalibrations. This was the largest source of uncertainty in the experiment.

Due to the finite divergence of the laser beam (solid angle $\Delta\omega_L$) and the geometry of the test detector, it was impossible to distinguish between transmitted radiation and radiation forward scattered within an angle of 10° to the incident beam direction. Thus, the phase function is arbitrarily set to zero in this interval. Houston [7] has shown that scattering within this narrow forward angle can be considered as transmission without significant effect on the predicted radiant heat flux.

Due to the finite thickness of the sample, radiation from the incident laser beam which is scattered within the sample can be partially absorbed or rescattered before leaving the sample. To account for this, the equation of transfer was solved for the intensity of radiation leaving the sample. In general, the equation of transfer is,

$$\frac{dI_\lambda(s)}{ds} = -(\alpha_\lambda + \sigma_{s\lambda})I_\lambda(s) + \alpha_\lambda I_{b\lambda}(s) + \frac{\sigma_{s\lambda}}{4\pi}\int_{w'=4\pi} I_\lambda(s, w')\Phi_\lambda(w, w')\,dw'. \quad (2)$$

The chopper and lock-in amplifier will eliminate radiation emitted by the sample. Radiant energy scattered at angles greater than 10°, i.e. out of the initial included angle of the laser, may be rescattered back into the laser beam or into another direction. The contribution of rescattering will be assumed negligible; this can be verified by calculations using the measured phase function. These assumptions serve to simplify the solutions to the equation of transfer. Within the initial divergence angle of the laser, the laser intensity can be found as:

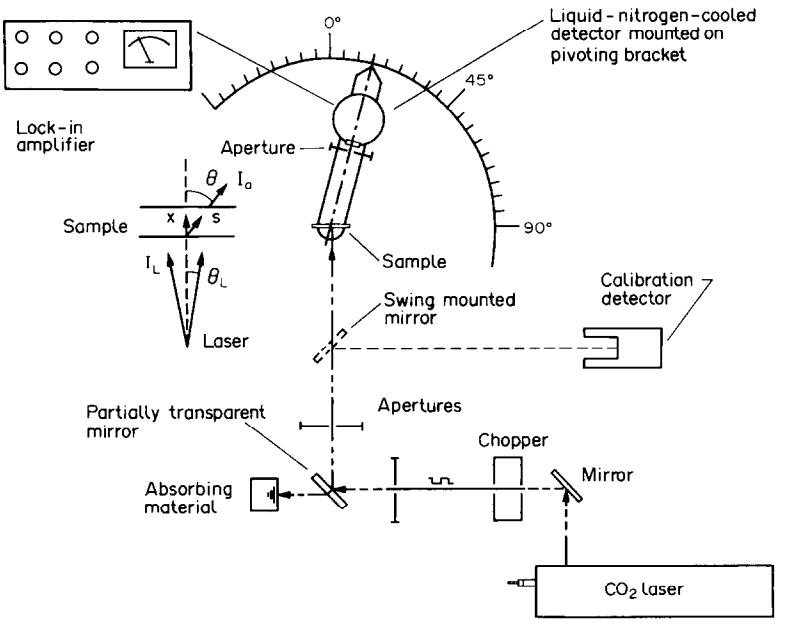

FIG. 2. Scattering experiment apparatus.

$$\theta \leqslant \theta_L$$
$$\frac{I_{L(x)}}{I_{L0}} = \exp\{-(\alpha+\sigma_s)x\} \tag{3}$$

where the subscripts λ have been omitted for simplicity. At larger angles, the only appreciable contribution is due to scattering from the original laser beam direction. The equation of transfer (neglecting emission and in scattering from all directions except the initial laser divergence angle) becomes:

$$\frac{dI(s)}{ds} = -(\alpha+\sigma_s)I(s) + \frac{\sigma_s}{4\pi}[I_L(x)\Phi(\theta)\Delta\omega_L] \tag{4}$$

where $I(s)$ is the intensity at angle θ and distance s from the front surface of the sample when the laser is incident.

Equation (3) allows the extinction coefficient to be determined from measurements of intensity leaving the sample in the initial laser direction. Equations (3) and (4) can be combined to relate the measured intensity leaving the sample at larger angles, $I_m(\theta)$, to the phase function and the scattering coefficient, Schuetz [8]. The result becomes,

$\theta_L < \theta < \pi/2$:

$$\frac{I_m(\theta)}{I_0\Delta\omega_L} = \frac{\sigma_s\Phi(\theta)}{4\pi(\alpha+\sigma_s)(1-\cos\theta)} \times \{e^{-(\alpha+\sigma_s)t} - e^{-[(\alpha+\sigma_s)t]/\cos\theta}\}. \tag{5}$$

$\pi/2 < \theta < \pi$:

$$\frac{I_m(\theta)}{I_0\Delta\omega_L} = \frac{\sigma_s\Phi(\theta)}{4\pi(\alpha+\sigma_s)(1-\cos\theta)} \times \{1 - e^{-(\alpha+\sigma_s)t[1-(1/\cos\theta)]}\} \tag{6}$$

where t is the thickness of the sample. Using $(\alpha+\sigma_s)$ from equation (3), the product $\sigma_s\Phi(\theta)$ may be determined at each angle, θ, from $I_m(\theta)$ and equations (5) and (6). Normalization of $\Phi(\theta)$ over all angles allows the phase function and scattering coefficient to be determined from the product $\sigma_s\Phi(\theta)$.

EXPERIMENTAL RESULTS

Transmission through foam sample

Figure 3 shows a typical result for the spectral transmission through a typical polyurethane foam sample (density of 32 kg m^{-3}) measured with a conventional spectrometer. The variation of the extinction coefficient with wavelength is noticeably less than that observed for a single cell wall. The difference is due to the influence of the struts, formed at the junction of the cell walls, which have been found to contain a majority of the polymeric material; see Reitz *et al.* [2]. The characteristics shown on Fig. 3 were found on numerous other foam samples, leading to the simplification of the foam as a gray body with an extinction coefficient approximately constant over wavelength. Figure 4 shows the wavelength average transmission measured for nine samples of different thickness taken from the same foam slab. The slope of the straight line permits a determination of the extinction coefficient from equation (3). For the sample of Fig. 4, the measured extinction coefficient was found to be 15.8 cm^{-1} (40 in.$^{-1}$). Note that the sample thickness less than 0.5 mm were not tested since such samples would be smaller than typical cell diameters within the foam.

Stern [9] used this technique to measure the extinction coefficients of four foam samples: two polyurethanes, one polyisocyanurate, and one polystyrene

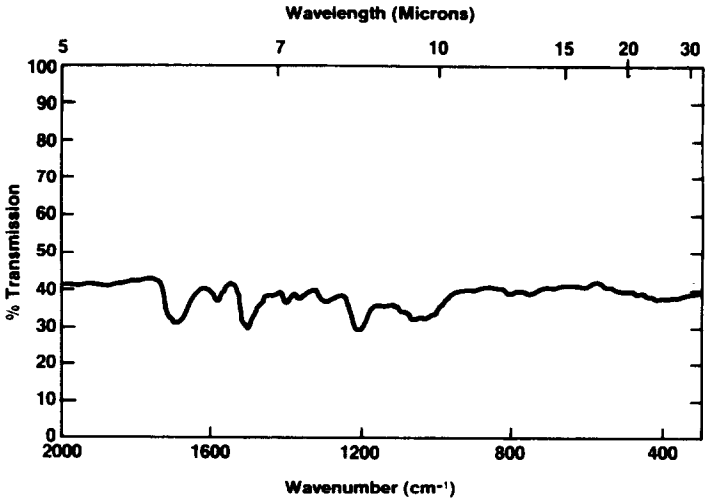

FIG. 3. Transmission through 0.55-mm-thick polyurethane foam sample.

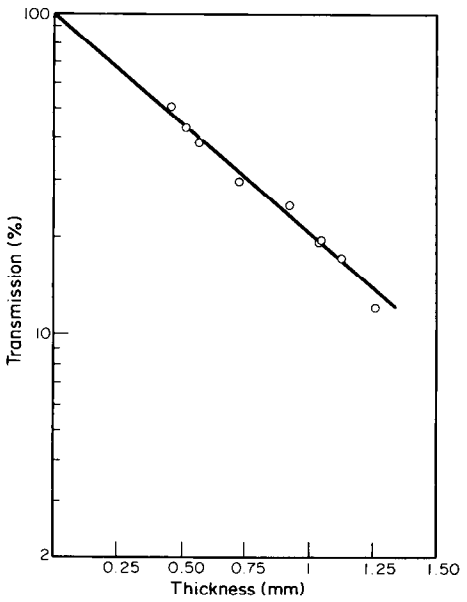

FIG. 4. Data for 32 kg m^{-3} polyurethane foam extinction coefficient measurement.

foam. The results ranged from 20.4 cm^{-1} (52 $in.^{-1}$) for a 28 kg m^{-3} (1.77 lb ft^{-3}) polyurethane foam to 42.5 cm^{-1} (108 $in.^{-1}$) for a 43 kg m^{-3} (2.68 lb ft^{-3}) polyurethane foam. The author's own data for a series of polyurethanes of density 29.6–55.2 kg m^{-3} (1.85–3.45 lb ft^{-3}) ranged from 14.2 to 24.7 cm^{-1} (36 to 63 $in.^{-1}$), respectively. For this set of samples of fixed foam chemistry (lower density samples were obtained by simply adding more blowing agent to the batch), the extinction coefficient was found to be linearly proportional to foam density. Based on the measured extinction coefficients, the optical thickness (the product of the extinction coefficient and the sample thickness) is greater than 10 for sample thicknesses greater than 7 mm (0.28 in.).

This experimental technique has been found to work consistently when the foam is homogeneous. However, if the cell size distribution is wide or if filler materials are added to the foam and are not uniformly dispersed, a larger number of data points are required to achieve a statistically accurate average value.

The results of the scattering measurements for polyurethane foam and fiberglass are shown on Figs. 5 and 6, respectively. For the foam, four different sample thicknesses were used ranging from 0.55 to 2.11 mm. The values of a_λ, $\sigma_{s\lambda}$, and $\Phi_\lambda(\theta)$ were found by using the data reduction procedure described earlier. As mentioned earlier, $\Phi(0)$ was taken to be zero for angles less than 10°.

At a given angle, the standard deviation of the measured phase function for the different thicknesses ranges from about 10 to 30% of the mean.

The absorption and scattering coefficients given in Figs. 5 and 6 were derived from the scattering experiment. The extinction coefficient for the foam was found to be 19.7 cm^{-1}. When the transmissivities of the same foam samples were measured in a conventional spectrometer, the extinction coefficient was found to be 20.9 cm^{-1}. Measurements made from the two techniques must be compared with care since they are not measuring the identical property. More will be said of this later.

For foam and other materials such as fiberglass, scattering makes a substantial contribution to the extinction. In order to identify the cause of scattering in the foam, the scattering experiment was repeated with the foam sample replaced by a single cell wall of a free rise sample. In the incident angle of the laser, the detected intensity fell by approximately 50%. For angles between 10° and 90°, the total scattered energy represented less than 0.5% of the incident energy. Thus, the film absorbs radiant energy but does not scatter appreciable radiation. These results were found when the film was normal to the incident laser

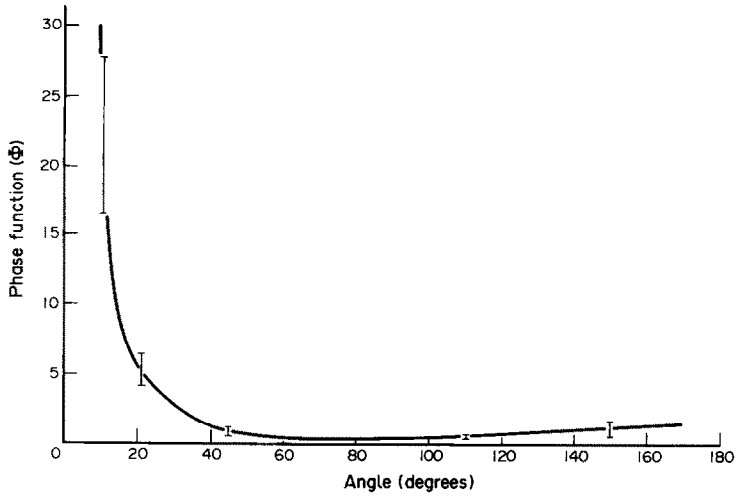

FIG. 5. Properties of polyurethane foam 28.2 kg m^{-3} (1.76 lb ft^{-3}) measured at 9.64 m narrow wavelength. Average absorption coefficient 14 cm^{-1} (427 ft^{-1}); average scattering coefficient 5.7 cm^{-1} (175 ft^{-1}). Bars on graph indicate standard deviation of data measured at four sample thicknesses between 0.0546 cm (0.0125 in.) and 0.021 cm (0.083 in.).

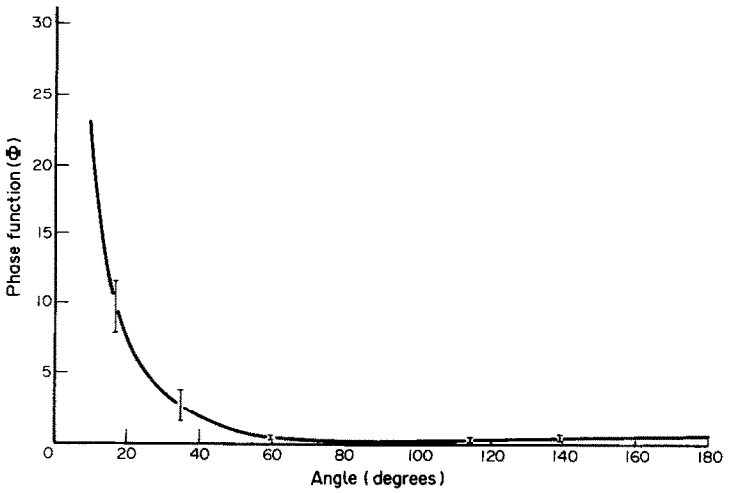

FIG. 6. Properties of glassfiber insulation 10.1 kg m^{-3} (0.63 lb ft^{-3}). Measured at 9.64 μm wavelength. Average absorption coefficient 3.2 cm^{-1} (98 ft^{-1}); average scattering coefficient 3.5 cm^{-1} (106 ft^{-1}). Bars on graph indicate standard deviation of data measured at two sample thicknesses, 0.23 cm (0.126 in.) and 0.39 cm (0.154 in.).

beam. Similar results were found at angles of 75°, 60° and 45° to the incident beam. Thus, scattering must be caused by radiation interaction with the struts in the foam.

APPLICATION TO THEORY

Based on the measured properties of insulation, a simplified model to predict the heat transfer through the insulation can be verified. In addition, a simplified method will be evaluated to measure the properties required by the heat flux calculation.

The measurements of foam and low density fiberglass insulation resulted in extinction coefficients of about 20 and 7 cm^{-1}, respectively. Thus, 2.5-cm (1-in.) thick, samples of foam and fiberglass will have optical thicknesses of 50 and 18, respectively. This suggests that radiative transfer in most commercially important thicknesses of insulation can be treated as optically thick, enabling use of a diffusion approximation.

The Rosseland equation should be valid when the insulation absorbs and isotropically scatters [10]. For one-dimensional heat flux

$$q_r = \frac{-4}{3K_R}\frac{de_b}{dx} = -\frac{16\sigma T^3}{3K_R}\frac{dT}{dx} \tag{7}$$

where K_R is the Rosseland mean extinction coefficient. The radiative flux can be added to the flux due to conduction through the gas and the polymer forming the cell to yield the total heat flux

$$q = -k_c \frac{dT}{dx} - \frac{16\sigma T^3}{3K_R} \frac{dT}{dx}. \quad (8)$$

Fine *et al.* [11] solved the equation of transfer [equation (2)] for an *isotropically scattering* gray medium and compared the resulting heat flux to the predictions using the Rosseland approximation [equation (8)]. At an optical thickness of 17, the radiant flux varies by 3.5% when the albedo (the ratio of scattering to extinction coefficient) varies between zero and unity. The influence of the albedo is smaller at higher optical thickness. For combined conduction and radiation with an albedo of 0, and bounded by surfaces with an emissivity of 1.0, the error in the calculated flux using equation (8) is approximately 5% of the radiation flux at an optical thickness of 8.3. Higher albedo and lower boundary emissivity increases the error somewhat. The error is due to the use of the Rosseland equation near the surface of the insulation. At larger optical thickness, the error becomes negligible.

When the medium is not gray, the Rosseland equation can still be used as long as the optical thickness at every wavelength is much greater than unity. In this case, the Rosseland mean absorption coefficient is used

$$\frac{1}{K_R} = \int_0^\infty \frac{1}{K_\lambda} \frac{\partial e_{b\lambda}}{\partial e_b} d\lambda. \quad (9)$$

The scattering measurements have shown that scattering by both foam and fiberglass are highly anisotropic. If the Rosseland equation is used for this case with the measured extinction coefficient, there will be considerable errors in the predicted heat flux.

A weighted scattering coefficient, the $P-1$ approximation, has been suggested to account for anisotropic scattering [10, 12]

$$\sigma_{s\lambda}^* = \sigma_{s\lambda}(1 - \langle \cos\theta \rangle_\lambda) \quad (10)$$

where

$$\langle \cos\theta \rangle_\lambda = 0.5 \int_{-1}^{1} \Phi_\lambda(\theta) \cos\theta \, d(\cos\theta). \quad (11)$$

The weighted monochromatic extinction coefficient,

$$K_\lambda^* = \alpha_\lambda + \sigma_{s\lambda}^* \quad (12)$$

is then used in the solution for isotropic scattering media.

Lee and Buckius [12] have numerically shown for several assumed phase functions that the modified extinction coefficient gives accurate results for the heat flux.

A trial calculation was made for a 3.8-cm (1.5-in.) thick foam and a 3.8-cm (1.5-in.) thick fiberglass insulation with the properties measured in this study. The heat flux predicted using equations (8) and (12) was compared to the numerical solution of the equation of transfer using the detailed phase function. The latter calculation was carried out by Koram [13] using a computer program written by him. The solution for the heat flux predicted by the $P-1$ approximation and the complete numerical solution agreed to within 1%. Thus, use of the $P-1$ approximation with the diffusion equation will be valid for insulations of moderate or large optical thickness.

MEASUREMENT OF WEIGHTED EXTINCTION COEFFICIENT

Although the $P-1$ approximation yields an accurate prediction of the radiant flux, it requires detailed measurements of the phase function which may also vary with wavelength. The usefulness of the approxi-

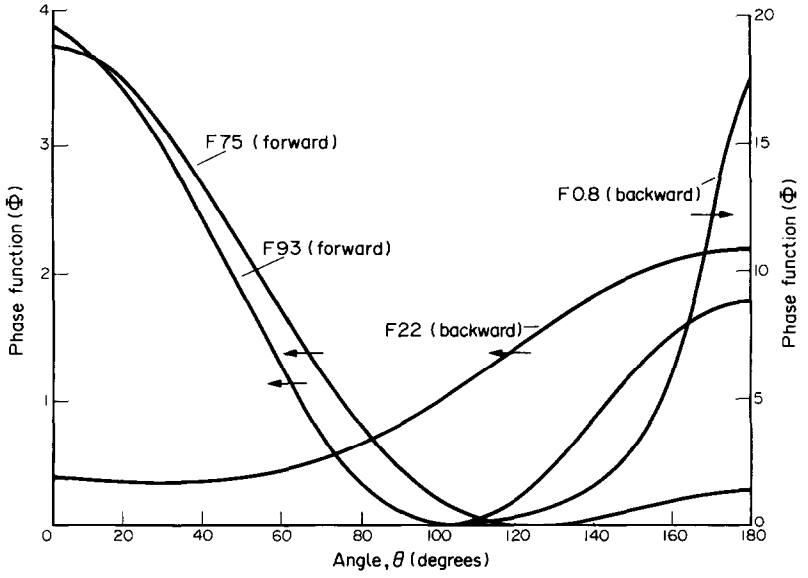

FIG. 7. Assumed phase functions.

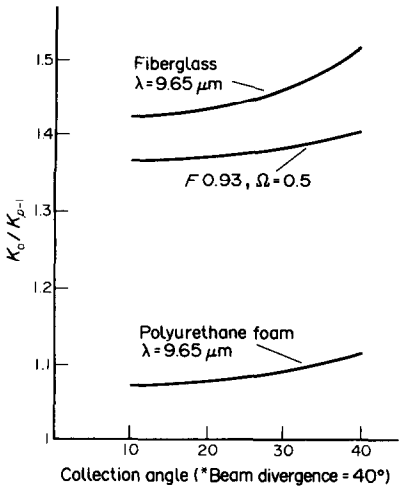

FIG. 8. Numerical simulation results for measured extinction coefficient vs collection angle.

mation for a real material requires a simple technique to measure the weighted extinction coefficient. It is not *a priori* clear under what conditions the extinction coefficient measured with a conventional spectrometer will be an adequate approximation to the weighted extinction coefficient.

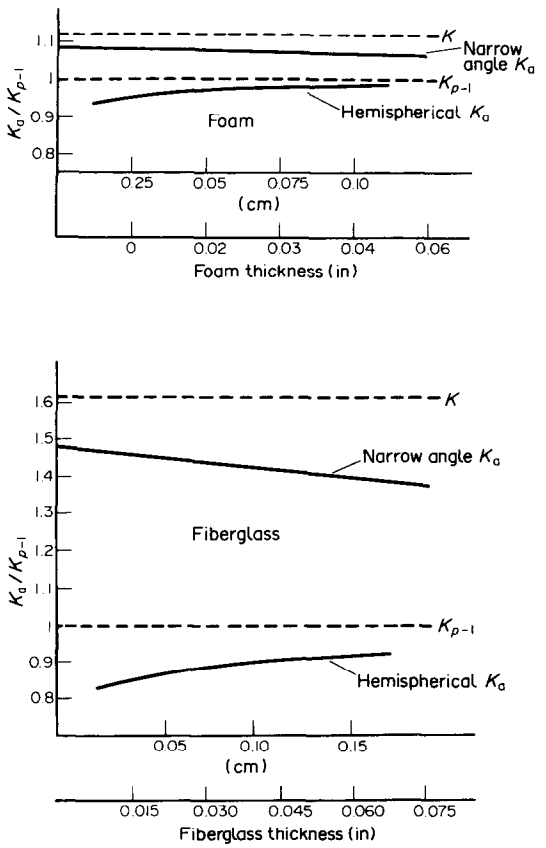

FIG. 9. Numerical simulation results for measured extinction coefficient using narrow angle and hemispherical detectors compared to the weighted or $P-1$ extinction coefficient, equation (12), for foam and fiberglass.

A numerical solution for combined absorption and scattering within a sample was used to examine the accuracy of several simplified measurement techniques. The computer program numerically solves the equation of transport for a gray absorbing, anisotropically scattering, planar medium with boundary conditions similar to those occurring in a typical infra-red spectrometer. Radiant energy of a given beam divergence is incident on one face; while the energy leaving the other face is integrated within a specified solid angle to simulate the optics of the infra-red collector. The equation of transfer, equation (2), was simplified by omitting energy emitted by the sample and assuming spherical symmetry. The simplified equation of transfer may be expressed in difference form as

$$I(x+\Delta x,\theta) = I(x,\theta)\left[1-(\alpha+\sigma_s)\frac{\Delta x}{\cos\theta}\right] + \frac{\sigma_s \Delta x}{2\cos\theta}\sum_{\theta'=0}^{\pi} I(x,\theta')\Phi(\theta,\theta')\sin\theta'\,\Delta\theta' \quad (13)$$

with the phase function expressed as a Legendre polynomial expansion. Equation (13) is numerically solved by stepping through the medium from the surface where the sample beam is incident, $x = 0$, to the opposite surface, $x = L$. To account for backscattering, the stepping process is then reversed from L to 0 to determine the intensity of energy scattered at angles greater than $\pi/2$. The stepping from 0 to L is then repeated.

Calculations were carried out for the measured phase functions of foam and fiberglass, shown on Figs. 5 and 6, as well as several assumed phase functions shown on Fig. 7. In the figures, the forward fraction, F, is defined as

$$F \equiv \frac{\int_0^{\pi/2} \Phi \sin\theta\, d\theta}{\int_0^{\pi} \Phi \sin\theta\, d\theta}. \quad (14)$$

For our discussion, a 'forward scattering' material has F greater than 0.5 while a 'backward scattering' material has F less than 0.5.

For the measured properties of foam and fiberglass, inclusion of backscattering had only a small effect on the calculated total intensity leaving the face of the sample at $x = L$. An apparent extinction coefficient may be defined as the slope of the logarithm of total hemispherical transmissivity vs sample thickness. For the measured phase functions of foam and fiberglass, when backscattering was neglected, the apparent extinction coefficient varied by 0.5% or less compared to when backscattering was included. For three of the other assumed phase functions (shown on Fig. 7), $F75$, $F50$ and $F22$, exclusion of the backscattering caused, at most, a 6% change in the apparent extinction coefficient at an albedo of unity. For lower values

Table 1. Numerical simulation results for measured or apparent extinction coefficient, K_a, compared to the scaled extinction coefficient, K_{P-1} for phase functions shown on Fig. 7

Phase function	Albedo	Optical thickness	K_a/K_{P-1} Narrow angle detector	K_a/K_{P-1} Hemispherical detector
*F*93	0.25	1.0	1.16	0.99
		2.0	1.16	1.01
	0.5	1.0	1.37	0.92
		2.0	1.36	0.99
	0.75	1.0	1.65	0.77
		2.0	1.61	0.88
*F*75	0.25	1.0	1.09	0.98
		2.0	1.09	1.0
	0.5	1.0	1.17	0.88
		2.0	1.16	0.91
	0.75	1.0	1.25	0.74
		2.0	1.23	0.8
Isotropic	0.25	1.0	1.01	1.0
		2.0	1.01	1.0
	0.5	1.0	1.01	0.9
		2.0	1.01	0.92
	0.75	1.0	1.01	0.78
		2.0	1.01	0.89
*F*22	0.25	1.0	0.92	0.96
		2.0	0.92	0.97
	0.5	1.0	0.85	0.83
		2.0	0.85	0.85
	0.75	1.0	0.80	0.7
		2.0	0.80	0.72
*F*8	0.25	1.0	0.85	0.9
		2.0	0.85	0.94
	0.5	1.0	0.74	0.74
		2.0	0.74	0.8
	0.75	1.0	0.66	0.6
		2.0	0.66	0.68

of the albedo, the influence of backscattering was less. Therefore, in all of the succeeding calculations, backscattering was omitted. That is, the numerical calculations marched from $x = 0$ to L, but did not step back to $x = 0$ as previously described.

As a further check on the calculations, the results were compared to those of Lee and Buckius [12] for a diffuse radiant source incident on the sample boundary, and to those of Evans *et al.* [14] for a collimated radiant source incident on the boundary. The results for the transmissivity agreed with the former to within 4% of the total value for an albedo of 0.9 and an optical thickness of 2 and 5 and within 2% for an albedo of 0.7 and an optical thickness of 2. The latter results agreed with the Evans *et al.* results for optical thickness between 0.25 and 1.0 and an albedo of 0.9 within an average difference of 1.7% for the calculated transmissivity.

Once verified, the computer program was used to simulate the results obtained with conventional laboratory instruments and determine their suitability to approximate the modified $P-1$ extinction coefficient. A standard laboratory infra-red spectrometer such as the Perkin–Elmer 283B nominally has both small beam divergence and collection angle, both angles being in the range 15–40° [15]. Because of the required spectral resolution from the dispersing element, slits are used which typically cause the collection angle to be smaller than the beam divergence.

Figure 8 shows the effect of detector collection angle on the ratio of the measured to the scaled or $P-1$ extinction coefficient for foam and fiberglass. In all cases presented, the collection angle is smaller than the incident beam divergence. For polyurethane foam, the difference between the measured extinction coefficient and the scaled $P-1$ coefficient was found to range from 5 to 12%. For glassfibers, there were considerably larger differences (35–65%).

Measurements which give a closer indication of the net transmission through the sample of both transmitted and scattered energy should result in a better estimation of the scaled or $P-1$ extinction coefficient. Figure 9 shows a comparison of the measured extinction coefficient when the transmissivity is measured on a spectrometer with either a narrow angle detector or a hemispherical collector. The hemispherical collector collects the energy leaving the back face of the sample at every angle. The 'transmissivity' is taken to be the ratio of the incident energy to the detected energy. The extinction coefficient is calculated from

the slope of the line of log transmissivity vs sample thickness. For foam, either technique (hemispherical or narrow angle) gives an acceptable measure of the scaled or $P-1$ extinction coefficient, although the hemispherical is more accurate at larger sample thickness. For fiberglass, the narrow angle measurement is unacceptable whereas the hemispherical measurement yields a good estimate of the scaled extinction coefficient. Note that both the narrow angle measurement and the hemispherical measurement vary somewhat with sample thickness. Anisotropic scattering causes the observed transmissivity to deviate slightly from exact exponential decay.

Similar calculations were made for the assumed phase functions shown on Fig. 7. The results are summarized in Table 1. Note that for forward scattering materials, $F > 0.5$, with substantial absorption, an albedo of 0.5 or less, the extinction coefficient derived from hemispherical measurements gives a good approximation to the weighted extinction coefficient. Also, the weighted extinction coefficient is bracketed by the two measurements. For backscattering insulations, $F22$ and $F8$, the measurements do not give a good estimate of the scaled coefficient when the albedo is high. Fortunately, no known insulation exhibits such behavior. However, caution must be used when applying the approximate measurements described in this paper to totally new materials. Additional details on the theoretical analysis of extinction coefficient measurements may be found in Sinofsky [16].

CONCLUSIONS

Polyurethane insulations are not opaque to infrared radiation. Cell walls have a transmissivity greater than 0.8. Radiation is a significant heat transfer mechanism for foam insulations at room temperature. Reducing the transmissivity can have a substantial impact on the overall conductivity of foams. Foam insulation one quarter inch or thicker can be considered optically thick such that radiative transfer may be modeled as a diffusion process.

Foam scatters radiation in an anisotropic fashion, due to the interaction of the radiation with the struts, although scattering is far more important in fiberglass than in foam insulation.

The radiative heat transfer through foams and fiberglass can be accurately modeled by the use of a scaled or $P-1$ extinction coefficient combined with the Rosseland equation.

For foams, the weighted extinction coefficient can be determined within 10% from transmission measurements on a conventional infra-red spectrometer such as the Perkin–Elmer 283B. For forward scattering materials with a large albedo, such as fiberglass, transmission measurements using a hemispherical collection system is needed to give a satisfactory estimate of the scaled or $P-1$ extinction coefficient. Detailed measurements of the scattering phase function vs angle is unnecessary. A material with strong backscattering will give erroneous results for the scaled extinction coefficient if experimental techniques that rely on transmission measurements are used.

For any unknown fibrous insulation, it may be simplest to measure the scaled extinction coefficient and compute the radiant flux using the diffusion approximation. Radiative calculations more detailed than the diffusion approximation are not justified until detailed measurements of the radiative properties are performed.

Acknowledgments—This work was carried out at MIT under funding by the Department of Energy under the Energy Conservation and Utilization Technology program (ECUT), through Oak Ridge National Laboratory. The assistance and suggestions of J. Carpenter, D. McElroy and W. Rohsenow are acknowledged. Use of facilities and technical assistance in the laser scattering experiment was provided by the MIT Regional Laser Center, courtesy of the National Science Foundation. We are indebted to Dr K. Koram for carrying out numerical solutions of the equation of transfer.

REFERENCES

1. M. A. Schuetz and L. R. Glicksman, A basic study of heat transfer through foam insulation, *J. cell. Plast.* **20,** 114–121 (1984).
2. D. Reitz, L. R. Glicksman and M. A. Schuetz, A basic study of aging of foam insulation, *J. cell. Plast.* **20,** 104–113 (1984).
3. R. E. Skochdopole, The thermal conductivity of foamed plastics, *Chem. Engng Prog.* **57,** 57 (1961).
4. D. C. Doherty, R. Hurd and G. R. Lester, The physical properties of rigid polyurethane foams, *Chem. Ind.* 1343 (1962).
5. J. A. Valenzuela and L. R. Glicksman, Thermal resistance and aging of rigid urethane foam insulation, *Proc. DOE–ORNL Workshop on Mathematical Modeling of Roofs*, Atlanta, GA, Conf-811179, pp. 261–262 (1981).
6. R. J. J. Williams and G. M. Aldao, Thermal conductivity of plastic foams, *Polym. Engng Sci.* **23,** 293–298 (1983).
7. R. L. Houston, Combined radiation and conduction in a nongray participating medium that absorbs, emits, and anisotropically scatters. Ph.D. thesis, Ohio State University, Columbus, OH (1983).
8. M. A. Schuetz, Heat transfer in foam insulation. M.S. thesis, Massachusetts Institute of Technology, Cambridge, MA (1982).
9. C. H. Stern, Radiation characteristics of rigid foam insulation. B.S. thesis, Massachusetts Institute of Technology, Cambridge, MA (1982).
10. H. C. Hottel and A. F. Sarofim, *Radiative Transfer*, pp. 326–342; 20–24. McGraw-Hill, New York (1967).
11. H. A. Fine, S. H. Jury, D. W. Yarbrough and D. L. McElroy, Analysis of heat transfer in building thermal insulation, ORNL/TM-7481 (1980).
12. H. Lee and R. O. Buckius, Scaling anisotropic scattering in radiation heat transfer for a planar medium, *J. Heat Transfer* **104,** 68–75 (1982).
13. K. K. Koram, Owens-Corning Fiberglas Corporation, Personal communication (1982).
14. L. B. Evans, C. M. Chu and S. W. Churchill, The effect of anisotropic scattering on radiant transport, *J. Heat Transfer* **87,** 381–387 (1965).
15. R. Anacreon, Perkin–Elmer Scientific Instruments, Personal communication (March 1983).
16. M. Sinofsky, Property measurement and thermal performance prediction of foam insulations. M.S. thesis, Massachusetts Institute of Technology, Cambridge, MA (1984).

TRANSFERT RADIATIF DE CHALEUR DANS L'ISOLATION PAR MOUSSE

Résumé—On examine la contribution du rayonnement thermique dans la conductivité globale des isolants poreux. Les coefficients d'absorption et de diffusion aussi bien que la fonction de phase sont mesurés pour l'isolation par une mousse et par fibres de verre. Un coefficient d'absorption simple peut être dérivé des mesures de transmission pour un certain domaine d'épaisseur. Quand ce coefficient d'absorption est utilisé dans l'équation de diffusion pour prédire le flux radiatif, l'erreur dans le calcul du flux est de l'ordre de dix pourcent pour les mousses. Pour les isolants fibreux, des mesures de transmittivité avec une sphère intégrante sont nécessaires.

WÄRMEAUSTAUSCH DURCH STRAHLUNG IN ISOLIERUNGEN AUS SCHAUM

Zusammenfassung—Es wurde der Strahlungsanteil am gesamten Wärmedurchgang in Isolierungen aus Schaum untersucht. Die Absorptions- und Streuungskoeffizienten sowie die Phasenfunktion wurden für schaumförmige und faserige Isolierungen gemessen. Ein einfacher Absorptionskoeffizient kann durch Transmissions-Messungen an verschieden dicken Proben hergeleitet werden. Wenn dieser Absorptionskoeffizient verwendet wird, um den Wärmestrom durch Strahlung an Schäumen vorherzusagen, liegt der Fehler des berechneten Wärmestroms durch Strahlung im Bereich von 10 Prozent. Für faserige Isolierungen sind die Transmissionsmessungen über den Raumwinkel integrierend durchzuführen.

ЛУЧИСТЫЙ ПЕРЕНОС В ПЕНОИЗОЛЯТОРЕ

Аннотация—Изучается вклад лучистого переноса в общую теплопроводность пеноизоляторов. Измерены коэффициенты поглощения и рассеяния, а также фазовая функция для пенистых и стекловолоконных изоляторов. Коэффициент поглощения может быть определен из измерений коэффициента пропускания в некотором диапазоне толщин образца. При использовании коэффициента поглощения в уравнении диффузии для расчета радиационного потока для пен, ошибка составляет порядка 10%. Необходимы измерения интегрального пропускания для волоконной изоляции.